THE UNIVERSITY OF

WARWICK

Density functional theory calculations of adsorption-induced surface stress changes

M.J. Harrison, D.P. Woodruff[*] and J. Robinson

Physics Department, University of Warwick, Coventry CV4 7AL, UK

Abstract

Density functional theory calculations of adsorbate-induced surface stress changes have been performed for a number of adsorbate and overlayer systems for which experimental data exists, namely: oxygen and sulphur adsorption on Ni(100); oxygen adsorption on W(110); pseudomorphic growth of Ni on Cu(100) and of Fe on W(110); oxygen adsorption on a 5 ML pseudomorphic film of Ni(100) grown on Cu(100). The theoretical calculations reproduce all the qualitative features of the experimental data, but there are some significant quantitative differences, most notably for the two atomic adsorbates on the bulk Ni(100) surface, for which the theoretical stress changes are substantially smaller than the experimental ones, a situation not obviously attributable to experimental error. For the W(110)/Fe system there is also a marked difference between experiment and theory in the coverage at which key surface stress changes occur.

Keywords: Density functional calculations; chemisorption; surface stress; surface structure; nickel; copper; tungsten; iron; oxygen; sulphur; low index single crystal surfaces

[*] corresponding author. email d.p.woodruff@warwick.ac.uk

1. Introduction

While the equilibrium structure of surfaces is determined by the minimisation of the surface free energy, the role of one contribution to the energy, the surface stress, has been highlighted in some discussions of the factors determining quite a number of surface structures, particularly those involving reconstruction of the outermost surface layer(s) of both clean surfaces and some adsorbate-induced reconstructions. In most cases, however, these discussions are only qualitative, and there are rather few quantitative investigations of surface stress. Experimental studies of surface stress exploit the slight bending of a thin crystal 'beam' which occurs when the surface stresses on the two opposite faces are different; using a variety of methods to measure slight changes in the crystal curvature, the *change* in surface stress induced by adsorption on one face can be measured (e.g. [1]). This approach cannot, however, provide information on the absolute surface stress.

By contrast, the majority of theoretical calculations of surface stress have focussed on the absolute value of this quantity for clean surfaces (e.g. [2, 3, 4, 5, 6, 7, 8, 9, 10, 11, 12, 13], although there have also been a few calculations of adsorbate-induced surface stress changes [14, 15]. So far our own investigations of this type [16] have been concerned mainly with the specific cases in which substitutional adsorption leads to a surface alloy phase, and we have identified clear trends in the relationship of the calculated alloying-induced surface stress changes, the calculated and experimental atomic-scale 'rumpling' of the surface alloy layer, and the atomic radii of the alloying elements. One striking feature of the results of these calculations is that while alloying with adsorbate atoms having a larger atomic radius than that of the substrate atoms does lead to a reduction in the initial tensile surface stress of the clean surface, in some cases the stress change is so large that the absolute surface stress becomes compressive. Moreover, in one case investigated (Cu on W(100)) the adsorbate atom is smaller than the substrate atoms, yet alloying is still energetically favoured despite an *increase* in the tensile surface stress. These results are a timely reminder that relief of surface stress is not the only contribution to the surface free energy, and indeed that processes may even be favoured which *increase* the contribution of the surface stress to this total energy.

However, despite the interesting trends identified in these calculations, there is only one surface alloy phase for which there are experimental data on the alloying-induced surface stress change, with which to confront the theoretical calculations. For this one case, the Cu(100)c(2x2)-Mn surface phase, agreement between experimental [17] and calculated [18] values of this quantity is rather good, the discrepancy of about 20% being modest for a quantity which is both difficult to measure and difficult to calculate with great precision. For more conventional (low atomic number) chemisorption systems, there are quite a number of experimental surface stress change measurements, but few calculations. For the case of oxygen adsorption on Pt(111) [14], the agreement between theory and experiment is similar to that for the Cu(100)c(2x2)-Mn surface mentioned above. However, calculated stress changes associated with oxygen adsorption on Cu(100) in two different phases are about a factor of 3 larger than the experimental ones [19]; we have suggested that this large discrepancy may be due to effects of stress relief at antiphase domain boundaries in the experimental measurements on these surfaces. Calculated stress changes for oxygen (and carbon) adsorption on Ni(100) have also been reported [15]; these are discussed below in the context of our own results for the Ni(100)/O system.

In order to provide a more demanding test of theoretical surface stress calculations beyond these few examples, we have undertaken similar calculations for a range of different adsorption systems chosen specifically because experimental surface stress change measurements do exist. The specific systems investigated concern the adsorption of O on W(110) and Ni(100), the adsorption of S on Ni(100), the pseudomorphic growth of ultra-thin films of Ni(100) on Cu(100) and O adsorption on this resulting Ni surface, and the earliest stages of epitaxial growth of Fe on W(110). On W(110) one aspect of especial interest is the anisotropic surface stress of this two-fold symmetric surface. While our calculated surface stress changes reproduce essentially all of the qualitative trends of the experimental results, there are some significant quantitative discrepancies. Possible reasons for these discrepancies are discussed, including consideration of other relevant theoretical calculations. Coincidentally, of course, our DFT calculations also

provide quantitative information on the structural parameters associated with the lowest energy state of the surfaces, and these provide a further basis for comparison with experimental data.

2. Computational Details

The DFT calculations reported here were conducted using the CASTEP computer code [20], (version 3.02) with the aid of the Cerius graphical interface [21]. Except for the case of Ni growth on Cu(100), calculations were conducted on 7-layer double-sided slabs with inversion symmetry around the central layer of atoms, with all layers allowed to relax perpendicular to the slab relative to this central layer. With both faces of the slabs having identical adsorbate coverage the surface stress is the same on each face and it is particularly trivial to extract this quantity from the calculated three-dimensional stress tensor. The surface stress was calculated analytically, based on the Hellmann-Feynman forces. The W(110) surface calculations were performed using the centred rectangular Bravais unit mesh to ensure a diagonalised stress tensor from which the in-plane anisotropy in the [001] and [$\bar{1}$10] directions can be extracted directly. The lateral interatomic spacings within the slabs were fixed to the nearest neighbour value found in a similar DFT calculation for the bulk metals (using the same functionals and potentials); the associated bulk lattice parameters were 3.216 Å (W), 3.600 Å (Cu), 3.542 Å (Ni) and 2.816 Å (Fe).

For the calculations on the five-layer thick Ni films on Cu(100), the number of layers needed for a double-sided slab was found to be prohibitive with the computing resources available. In this case, therefore, single-sided slabs were used comprising 5 layers of Ni with two layers of Cu constrained to the bulk copper structure. This single-sided slab was then used to investigate O adsorption on the outermost Ni layer. In addition, further calculations to investigate this adsorption system were conducted on a 7-layer Ni slab, with the lateral interatomic spacing of Cu rather than Ni, to reproduce the consequence of the Cu epitaxy; on this slab single-sided calculations of the O adsorption were performed with the bottom two Ni layers fixed. Double-sided calculations of O adsorption were also

conducted on the 7-layer Ni slab with the lateral interatomic spacings of Cu, providing a check on the O-induced surface stress change on the Ni films.

All calculations were performed in the generalised gradient approximation (GGA) using PBE functionals [22] with a 380 eV cut off energy. *k*-point sampling used the Monkhorst-Pack scheme with a constant *k*-point spacing of less than 0.025 Å^{-1}. This is a significantly smaller spacing (by about a factor of 2) than would typically be used in calculations performed for geometry or adsorption energy optimisation, but we have found this finer sampling is essential for reasonable convergence of surface stress values which depend on energy and force gradients [16]. For W(110) this resulted in a 14x10x2 sampling grid, while for (1x1) and c(2x2) calculations on Ni(100) the sampling grids were 16x16x2 and 12x12x2 respectively.

3. Results and discussion
3.1 O and S adsorption on Ni(100) and W(110)

The surface stress changes associated with the formation of the c(2x2) adsorption phases of atomic O and S on Ni(100) provided some of the earliest measurements of adsorbate-induced surface stress changes [23, 1], while subsequently biaxial measurements of the surface stress change associated with a similar 0.5 ML oxygen coverage phase (in this case (2x1)) on W(110) seem to have provided the first data on anisotropic surface stress changes in oxygen adsorption [24].

Table 1 summarises the results of the present calculations of the absolute surface stress and adsorption-induced surface stress changes in these systems, and includes experimental values of these latter quantities. We should first remark on the values of the calculated surface stress for the clean surfaces for which the results of previous calculations have been published. In the case of Ni(100) for which our value is 2.22 N/m (positive, and thus tensile stress), the previously reported calculated values are 2.0 N/m and 3.0 N/m in recent DFT GGA and LDA calculations, respectively [15], and 1.27 N/m and 2.37 N/m from embedded-atom method (EAM) calculations [10, 11]. For Cu(100),

for which we report a value of 1.89 N/m, earlier calculations gave 1.38 N/m [10] and 1.40 N/m [11] in the same EAM calculations and 2.10 N/m [13] from a DFT slab calculation. Clearly our values are in the general range of previous calculations; we should emphasise that, as previously remarked both by us and other authors, the precision of surface stress calculations is generally much worse (probably no better than ~10%) than of other quantities derived from total energy calculations, such as adsorption energies and geometrical structural parameters, due to the more extreme demands of convergence and k-point sampling. Indeed, we should note that we have also previously reported a value of 2.39 N/m for the surface stress of Ni(100) and 1.51 N/m for Cu(100) in our studies of related surface alloy systems [16, 18]; the first of these values was obtained using an earlier version of CASTEP prior to improvements intended to render force calculations more reliable, while the second value did use the new version of the code and was also performed on 7-layer metal slabs in GGA using PBE functionals, but at that time the pseudopotentials available had been generated in LDA and not, as is the case in the pseudopotentials used here, in GGA. This difference in the combination of potential and approximation is known to lead to some differences in total energies [25] and also leads to a small difference in the bulk lattice parameter which may, at least in part, account for the different absolute surface stress value. A check of the Mn-induced surface alloy phase on Cu(100) using the new pseudopotentials showed that the surface stress *change* was almost unchanged by the use of the different pseudopotentials. For W(110) there is also one previous theoretical study based on a semi-empirical calculation [5], but the values of the surface stress reported, namely 0.27 N/m in the [001] direction and 2.29 N/m in the $[\bar{1}10]$ direction, differ very significantly from our values of 5.65 N/m and 3.75 N/m respectively. Not only is the quantitative value in the [001] direction very different, but the two calculations show opposite anisotropies. The methods of calculation are, however, very different, with our *ab initio* methods generally being regarded nowadays as substantially superior.

A comparison of the calculated and experimental adsorption-induced surface stress changes shows clear qualitative similarities. For example, all the adsorbate-induced stress changes are compressive, in both theory and experiment. For the W(110)/O system, both

6

theory and experiment show a much larger surface stress change in the $[1\bar{1}0]$ direction than in $[001]$. However, Table 1 also shows some significant quantitative discrepancies between theory and experiment. For the W(110)(2x1)-O surface (as for our earlier calculations for two different structural phases of oxygen on Cu(100) [19]), the theoretically calculated surface stress changes are very significantly larger than the experimentally observed values, but the opposite is true for the Ni(100)c(2x2)-S and Ni(100)c(2x2)-O systems.

Before considering the individual adsorption systems in more detail we discuss briefly possible sources of error in the experimental measurement. Of course, there may also be fundamental problems with the theoretical calculations, but these are more difficult to evaluate. There are at least two ways in which the experimental measurement may result in a value smaller than the true value. One, which is well-understood and generally surmountable, is the effect of adsorption on the back face of the sample. Clearly if the front and back faces adsorb at the same rate, the surface stresses on both faces change in identical fashion and there is no resultant bending and hence no apparent surface stress change. It is relatively straightforward to ensure that one face receives adsorbate dosing at a much higher rate than the other, largely overcoming this problem, although if the back face is similarly reactive, then as the front face saturates the relative rate of uptake of adsorbate on the back face can grow, so after long exposure times the initial bending may be lost as the two faces finally achieve the same adsorbate coverage. Typically, this problem can also be greatly reduced by ensuring that the back face of the crystal is in a much less reactive stat,e such as through contamination, and with the possible exception of the W(110)/O system ([26] see below), the published experimental data show no indication that this problem is significant. The second possible source of reduced measured values of the adsorbate-induced surface stress change is more fundamental. In calculating the surface stress we assume that the surface is perfectly ordered and effectively infinite in extent. In reality, an ordered adsorbate superstructure involves finite-sized domains on the surface in which the adsorbate ordering may be of high quality, but between these domains will be narrow regions of poor order, many of which are antiphase domain boundaries, with associated discontinuities in the long-range

ordering. Within these boundary regions (in which the local adsorbate coverage is expected to be lower) one might expect local adsorbate-induced stress relief to occur, so the average surface stress over the whole crystal is less than the stress within a single ordered domain – which corresponds to the quantity calculated theoretically. This problem was felt to be particularly relevant to the Cu(100)/O systems, for which there is clear prior evidence of domain boundary effects in the structures [19], but it is less clear that this is particularly important in the systems reported on here.

We now consider the individual adsorption systems in more detail. Bearing in mind that experimental difficulties are most likely to lead to reduced apparent surface stress changes, the most surprising result of Table 1 is the fact that the experimental adsorbate-induced surface stress changes for oxygen and sulphur adsorption on the surface of a bulk Ni(100) crystal are approximately a factor of 2 higher than the theoretically calculated values. It is particularly difficult to attribute this difference to any known intrinsic potential experimental limitation. Notice that the experimental values reported in the original study [23] were actually even higher than those in Table 1; the values shown here incorporate a later correction in the data analysis associated with the manner in which the samples were clamped [1]. The discrepancy between theory and experiment is greatest for the Ni(100)c(2x2)-O surface phase and it is interesting to note that an independent theoretical study of this system by Hong *et al.* has appeared very recently [15] and arrives at similar results to our own. Specifically, this work reports calculated oxygen-induced surface stress changes of –1.4 N/m and –1.6 N/m by two different (LDA) methods, even lower than our value of -2.60 N/m. Indeed, they also report the results of a GGA calculation, using the same PBE functional we have used, that yields an even lower surface stress change of only -0.8 N/m. Why this value is so different from our own is unclear, although there do appear to be significant differences in the details of the two calculations; Hong *et al.* report a need for a very high energy cut-off of 680 eV for the plane waves to be included, but use relatively coarse *k*-point sampling, whereas our own convergence tests have indicated the need for fine *k*-point sampling but a more conventional value for the high energy cut-off. In their paper Hong *et al.* show that the surface stress is rather sensitive to the interlayer spacing of the outermost Ni layer atoms

8

to the chemisorbed O atoms, and if they constrain this spacing to values lower than the one corresponding to the lowest total energy, the adsorbate-induced compressive surface stress change increases, and indeed can be increased to a value larger than that measured experimentally. One feature of both of these DFT calculations (our GGA and these earlier recent, mainly LDA, calculations) is that they both provide an excellent description of the equilibrium structure relative to experimental structural studies of these much-studied surfaces.

Table 2 shows a comparison of the optimised structural parameter values of all the surfaces reported in this section with experimental results. Interlayer spacings are denoted z_{ab} where a and b define the layers; the adsorbate is represented by its elemental name (O or S) and the substrate layers are numbered sequentially starting with 1 as the outermost layer. In some cases specific atoms in layers are given additional identifiers as described below. For the Ni(100)c(2x2)-O surface, the structure of which has been investigated experimentally by many methods over a long period of time, we show in Table 2 the results of the most recent quantitative LEED analysis, which also included an investigation of subsurface layer rumpling [27]. Due to problems of parameter coupling in LEED analysis, earlier investigations that failed to take account of these subsurface effects may contain consequential errors in the O-Ni interlayer spacing. The existence of second-layer rumpling means that two values are shown in Table 2 for the first-to-second Ni layer spacing, z_{12}, that corresponding to the layer spacing from the outermost layer to the second layer Ni atoms directly below the adsorbed O atoms being denoted z_{12A}, while that corresponding to the second layer Ni atoms not covered by O atoms is shown as z_{12B}. There is near-perfect agreement between our optimised DFT structure and the experiment in all the layer spacings and the rumpling amplitude. Similarly excellent agreement is found for the Ni(100)c(2x2)-S surface, although in this case even the most recent quantitative LEED analysis [28] (performed by the same group at much the same time as the Ni(100)c(2x2)-O analysis) did not consider the possibility of second layer rumpling, so we show only the average substrate interlayer spacings. In fact the second layer rumpling we find for the Ni(100)c(2x2)-S system is only half the amplitude (0.02 Å) of that found for the Ni(100)c(2x2)-O surface.

9

In the case of the W(110)/O system, for which the calculated surface stress change values are larger than the experimental values, a difference which could conceivably be related to stress relaxation and antiphase domain boundaries, the optimised structure is also in very good agreement with experimental structure determination, as shown in Table 2. There appears to be only one rather early quantitative LEED investigation of the W(110)(2x1)-O surface phase [29] that investigated only the O-W interlayer spacings, and not relaxation or rumpling of the substrate. Interestingly, our calculations show that while oxygen adsorption on Ni(100) and Cu(100) leads to an expansion of the outermost substrate layer spacing, on W(110) the outermost substrate layers show a significant contraction. It would be interesting to know if this can be confirmed experimentally. As noted above, the surface stress change measurements for oxygen adsorption on W(110) do show that with continued oxygen exposure the initial crystal bending associated with a compressive change in surface stress eventually attenuates to near zero, an effect attributed by the authors to oxygen adsorption on the back face of the crystal [26]. The shape of the crystal bending versus oxygen exposure plot found, with a rapid change at low exposure and a much slower decrease at high exposure, strongly suggests that the arrival rate at the back of the crystal is much lower than at the front, so the maximum bending seen is unlikely to be more than a few percent less than that characteristic of the total adsorbate-induced stress change. This effect is therefore far too small to account for the large quantitative discrepancy between the experimental and theoretical surface stress changes reported in Table 1. Nevertheless, it is notable that the strong anisotropy of the surface stress change of the calculations is consistent with that observed experimentally.

3.2 Pseudomorphic growth of Ni on Cu(100) and O adsorption

A rather interesting complement to the early measurement of the surface stress change associated with the formation of the Ni(100)c(2x2)-O phase, discussed in the previous section, is provided by very recent measurements associated with an investigation of pseudomorphic growth of Ni on Cu(100) and the role of adsorbed O as a surfactant [30]. This study involved measurement of the surface stress changes associated with the

10

pseudomorphic growth as a function of layer thickness, but also the stress change associated with exposure of pseudomorphically grown Ni(100) surface to produce a similar c(2x2)-O surface phase. There is no doubt that the most significant conclusions of this work relate to the nature of the oxygen surfactant layer when the Ni is grown onto a Cu(100) surface initially dosed with oxygen, but the experimental structure determination in this case indicates partial occupation of both surface and sub-surface oxygen sites together with surface roughening and some Ni/Cu intermixing. Realistic DFT slab calculations of this situation would require a very large supercell and are therefore beyond the scope of our present calculations. However, the experimental stress change data for oxygen dosing of the pseudomorphic layer grown on a clean Cu surface provide an interesting comparison of the influence of a c(2x2)-O overlayer on Ni(100) described in the previous section.

From the point of view of the surface stress change measurements, the experiments yield two main results. Firstly, for layer-by-layer growth of pseudomorphic Ni(100) on Cu(100), the stress change with coverage is tensile and linear, with a value of +0.65 N/m per ML for a coverage up to 8 ML. Our DFT calculations for a 5 ML thick film yield a total stress change of 4.11 N/m, corresponding to 0.82 N/m per ML, in quite good agreement. This increasing tensile stress is entirely consistent with the fact that the bulk Ni lattice parameter is smaller than that of the Cu substrate. The experiments show that adsorption of O on a 8 ML Ni film to form the c(2x2)-O surface phase leads to an experimental (compressive) surface stress change of -1.0 N/m. The DFT calculations (on a 5ML Ni film) yield a value for this parameter of -1.32 N/m, in reasonable agreement with the experiment, particularly when compared with the large experiment-theory discrepancy for the surface stress change associated with the formation of the c(2x2)-O surface phase on a bulk Ni(100) surface. Notice, too, that a consistent trend seen in both experiment and theory is that the compressive stress change associated with O adsorption on the pseudomorphic strained Ni(100) is much less than on the bulk Ni(100) surface; theoretically, there is a difference of a factor of 2, but experimentally the difference is a factor of 5.

The rationale for this large difference is not simple, not least because oxygen adsorption on the strained Ni(100) surface leads to differences in the structural parameters, as shown in Table 3. Previous total energy calculations for this system produced results very similar to those of Table 3. In particular, Hong *et al.* [31] have performed similar DFT calculations for several different thicknesses of pseudomorphic Ni on Cu(100) with and without a c(2x2)-O overlayer. They find the interlayer spacing within the film to be 1.75 Å, closely similar to our value and slightly reduced relative to the value for bulk Ni due to the tetragonal distortion of the pseudomorphic layer. On the clean surface, however, the outermost Ni-Ni layer spacing is substantially contracted to 1.64 Å, while the oxygen overlayer causes this to increase to 1.84 Å; both of these are closely similar to the values we report in Table 3. These authors also find the adsorbed oxygen induces a rumpling of the second Ni layer by 0.03 Å, essentially identical to our value of 0.04 Å, but do not report the O-Ni interlayer spacing. Some results of similar calculations have been reported by Nünthel *et al.* [32]; these authors specifically quote the value of the O-Ni interlayer spacing as 0.51 Å. While the qualitative trend for the O-Ni interlayer spacing to be less on the pseudomorphic Ni surface than on that of bulk Ni(100) is consistent with our own result (and with the expectation for a surface with a larger lateral Ni-Ni spacing), this numerical value is very significantly less than ours. There are experimental measurements of this parameter on the oxygen-covered surface of pseudomorphic Ni grown with the aid of an oxygen surfactant layer initially deposited on the Cu(100) substrate. Specifically, surface X-ray diffraction (SXRD) gives a value of 0.3-0.4 Å [30], while surface extended X-ray absorption fine structure (SEXAFS) measurements gave a value of 0.41 Å [33]. However, the SXRD study also provides clear evidence for a substantial amount of subsurface oxygen, and a very large outermost Ni layer rumpling (0.35 Å) associated with this underlying oxygen. As such this surface is quite different from the one we have modelled. Moreover, the conclusions of the SXRD study are that this subsurface oxygen is a characteristic of the oxygen surfactant layer and thus would also be present in the SEXAFS experiments. In this case, of course, the SEXAFS result (which is actually a measurement of the O-Ni nearest-neighbour distance, from which the layer spacing is inferred) would actually relate to an average property of the overlayer and subsurface oxygen species.

12

In considering the structural information of table 3, it is important to remember that the equilibrium *bulk* lattice parameters of Cu and Ni obtained from the DFT calculations differ from the true experimentally-determined values. Specifically, while the lattice parameters of Cu and Ni are 3.61 Å and 3.52 Å respectively (which differ by 2.5%), the values we find in our DFT calculations for the bulk solids are 3.60 Å and 3.54 Å (which differ by only 1.6%). Bearing in mind that this implies that the strain of the pseudomorphic Ni film is smaller in the DFT calculations than in reality, it is therefore surprising that the calculated tensile stress in the 5 ML film is actually slightly larger than that determined experimentally. A possible reason for this is an expected increasing roughness of the Ni film surface as it is grown without the aid of the oxygen surfactant.

3.3 Earliest stages of pseudomorphic growth of Fe on W(110)

There have been extensive investigations of the growth of the ferromagnetic 3d elements Fe, Co and Ni on W(110); like the Ni on Cu system described above, these are model systems of ultra-thin magnetic thin films, and some of this work has been accompanied by measurements of the associated changes in the associated stress (e.g. [34]). The growth of Fe on this surface has received particular attention, but it appears that pseudomorphic growth only occurs up to a coverage a little in excess of 1 ML; at higher coverages misfit dislocations appear in the film. Measurements of the surface stress change in this coverage range appear to reflect the effect of this structural change (Fig. 1). At the lowest (sub-monolayer) Fe coverages there is a slight decrease in the surface stress (i.e. the stress change is compressive – of the opposite sign to the tensile stress expected for the clean surface). With increasing coverage the stress change becomes tensile and rises sharply, reaching a local maximum at a coverage of 1.2 ML before dropping back and then rising more gradually as the average thickness increases to several atomic layers. Because the W(110) surface is only 2-fold symmetric, the surface stress is anisotropic, as discussed for the clean surface in section 3.1.

This anisotropy also leads to differences in the stress changes induced by Fe growth in

the two orthogonal directions. Fig. 1 summarises the experimental dependence of the surface stress on Fe coverage in the low coverage range; this figure is adapted from the later publication of the full experimental biaxial surface stress change measurements, allowing the component stress changes to be derived from the crystal bending in two orthogonal directions [26]; earlier reports of some of these measurements presented only crystal bending or uncorrected stress values [35, 24]. Also shown in fig. 1 are the results of our calculations of the surface stress change associated with the growth, these values being tabulated in Table 4. In addition to the calculation for a 1 ML pseudomorphic layer, and a 0.5 ML coverage layer which we assume to comprise an ordered (2x1) phase with the Fe atoms adopting the W continuation sites, we have also performed calculations for an ideal 2 ML pseudomorphic layer. The theoretical calculations reproduce the main qualitative trends of the experimental data, namely an initial compressive change in the surface stress which is larger in the [001] direction, followed at higher coverage by a much larger increase in the tensile surface stress that is larger in the [$\bar{1}$10] direction. However, the quantitative agreement is poor. One striking feature of this comparison, however, is that if the relative Fe coverage axis is changed by a factor of 2, the agreement between theory and experiment in the [$\bar{1}$10] direction is excellent; in the [001] direction the agreement is also significantly improved, although the magnitude of the compressive stress change at low coverage seen in the theoretical calculations is about a factor of 2 larger than in the experiment. The effect of this change in the relative coverages of the theoretical and experimental data is illustrated in fig. 1 by arrows displacing the theoretical values to one half of the actual coverages used in the calculations. Of course, while there may well be fundamental limitations in the theoretical calculations, the coverages used in them must be correct, so if there really was a discrepancy in coverage it must be the experimental coverages that are a factor of 2 too low. However, it is highly improbable that such a large error is present in the experimental coverage calibration, which was achieved by a variety of complementary methods. In particular, in addition to using vibrating quartz crystal thickness measurements, *in situ* surface X-ray diffraction to monitor the completion of layers in a layer-by-layer growth mode, together with simultaneous monitoring of the crystal bending [36], strongly implies that there can be no such large errors in the experiment.

14

While the difference in the coverage calibration suggested by the arrow-heads of fig. 1 therefore almost certainly does not have any basis in fact, the figure does show rather clearly that the qualitative trends of the experimental and theoretical surface stress changes with increasing coverage are very similar. Both show an initial compressive stress changing to an increasing tensile stress. Both show a larger compressive stress at low coverage in the [001] direction, and a smaller tensile stress in this direction at higher coverage. The large tensile stress in the theoretical calculation for the (hypothetically pseudomorphic) 2 ML film is also consistent with the fact that the substrate W(110) lattice parameter is much larger than that of bulk Fe; in the calculations the lateral Fe-Fe spacing is forced to be 2.785 Å, 14% larger than the equivalent value in bulk Fe of 2.439Å. Not surprisingly, the Fe-Fe interlayer spacing in this 2 ML film is only 1.87 Å, 0.12 Å smaller than in bulk Fe. At lower coverage, however, and particularly at sub-monolayer coverage, the calculations show that the behaviour is quite different, the local chemisorption (rather than lateral Fe-Fe attraction) leading to a compressive surface stress change. Quantitatively, however, the experimental and theoretical data of fig. 1 show rather important differences. In the [$\bar{1}$10] direction the theoretical surface stress changes are *smaller* than those measured experimentally. In the [001] direction, at the lowest coverage, the theoretical compressive stress change is *larger* than the experimental value. More significantly, perhaps, if we accept that the coverage calibration on both experiment and theory is correct, the coverage at which the switch from compressive to tensile stress changes occurs is different, the theory indicating that the compressive chemisorption behaviour is still the dominant effect, at least in the [001] azimuth.

4. Conclusions

There have been quite a number of publications dealing with theoretical calculations of surface stress, and of experimental adsorbate-induced surface stress changes, over the last 15 years, but there have been very few systems studied that allow direct comparison of

theory and experiment. Here we have presented the results of a series of new calculations of adsorbate-induced surface stress changes of a variety of systems for which experimental data exist: O and S on Ni(100), O on W(110), pseudomorphic growth of Ni on Cu(100) and the effect of O adsorption on the surface of the resulting strained Ni(100) film, and the earliest stages of pseudomorphic growth of Fe on W(110). In all cases the qualitative trends of the experimental results are reproduced by the DFT calculations: O and S adsorption in all cases lead to a compressive surface stress change; ultra-thin pseudomorphic films of Ni(100) and Fe(110), both grown on substrates with larger lattice parameters, lead to increasing tensile surface stress; the sign of the anisotropy of the surface stress changes on W(110) produced by both O and Fe is the same in theory and experiment; Fe growth on W(110) at sub-monolayer coverage leads to a compressive surface stress change. Despite all these successes, the quantitative agreement between theory and experiment, however, is generally not so good, with many cases in which they differ by a factor of two or more. In several cases the theoretical surface stress changes are larger than the experimental ones, and one possible contributory cause could be stress relaxation at antiphase domain boundaries in the experimental surfaces. However, for O and S adsorption on Ni(100), in particular, the measured surface stress changes are about a factor of two *larger* than the calculated values. Interestingly, recent independent calculations of the surface stress change associated with O adsorption on Ni(100) [15] lead to the same result; indeed, these calculations yield even lower calculated values than our own results.

Despite these substantial discrepancies in the experimental and theoretical values of the surface stress changes, theory and experiment are generally in excellent agreement regarding the structure of these surface phases. For the Ni(100)c(2x2)-O system, for which the discrepancy in the surface stress changes is large, there is extensive experimental data on the surface structure, and the agreement between experimental and theoretical structural parameters is essentially perfect. Of course, within the hierarchy of DFT methods it is generally accepted that it is much less demanding to arrive at the correct surface structure in an adsorption calculation, than to arrive at the correct adsorption energy. Bearing in mind that the surface stress depends on a derivative

function of the surface energy, it is therefore perhaps not surprising that getting the surface stress correct is even more demanding. One consequence of this that we have already identified is the need to use much finer k-point sampling than would normally be regarded as necessary to calculate the surface structure or the adsorption energy, in order to achieve reasonable convergence of the surface stress value. It may be that the choice of approximation and functional is also relevant to obtain the most reliable surface stress values. Of course, it would also be of interest to have a check on some of the experimental values. Ideally, one would like to have alternative methods of measurement, but while there are alternative methods to measure the adsorption-induced crystal bending, there seems to be no alternative to the basic strategy of measuring the macroscopic bending as a way of determining the surface stress changes.

Acknowledgements

Table 1. Summary of calculated absolute surface stress in Ni(100), Cu(100) and W(110) and for various O and S adsorption structures on these surfaces, together with both calculated and experimental adsorbate-induced surface stress changes.

Surface	Calculated surface stress (N/m)	Calculated adsorbate-induced surface stress change (N/m)	Experimental adsorbate-induced surface stress change (N/m)
Ni(100)	2.22		
Ni(100)c(2x2)-S	-0.98	-3.21	-5.0
Ni(100)c(2x2)-O	-0.38	-2.60	-5.4
Cu(100)	1.89		
W(110)	5.65 [001], 3.75 [$\bar{1}$10]		
W(110)(2x1)-O		-0.50 [001], -4.87 [$\bar{1}$10]	~0 [001], -1.12 [$\bar{1}$10]

Table 2

Comparison of the structural parameters of the lowest energy surface structures found in this study with experimental measurements of the same quantities for O and S adsorption phases on Ni(100) and W(110). * indicates a value for which layer rumpling (found in our calculations) was not tested in the experimental structure determination. The figures in parentheses are the fractional changes in interlayer spacing relative to the bulk values.

surface	parameter (all in Å)	this work	experiment
Ni(100)c(2x2)-O	z_{O1}	0.77	0.77±0.04 [27]
	z_{12A}	1.87 (+6%)	1.88±0.02 (+7%) [27]
	z_{12B}	1.83 (+3%)	1.84±0.02 (4%) [27]
	z_{23}(av.)	1.75 (-1%)	1.76±0.02 (0%) [27]
Ni(100)c(2x2)-S	z_{S1}	1.29	1.30±0.02 [28]
	z_{12}(av.)	1.79 (+2%)	1.79±0.02 * (+2%) [28]
	z_{23}(av.)	1.75 (-1%)	1.74±0.03 (-1%) [28]
W(110)(2x1)-O	z_{O1}	1.15	1.25±0.10 [29]
	z_{12}(av.)	2.20 (-4%)	bulk assumed? [29]

Table 3

Interlayer spacings for a 5 ML pseudomorphic film of Ni on Cu(100) with and without a c(2x2)-O overlayer, as determined in the present theoretical calculations. Also shown are comparable values of the Ni(100)c(2x2)-O surface as reported in Table 2. *in both the bulk Ni(100) and the pseudomorphic film O adsorption leads to a rumpling of the second Ni layer of 0.04 Å, with the Ni atom directly below the O atom lower in the surface (see table 2). The z_{12} and z_{23} values given for these structures are the *average* interlayer spacings.

layer spacing (all in Å)	5 ML Ni on Cu(100) – theory	5 ML Ni on Cu(100) + O – theory	Ni(100) + O - theory
z_{O1}	-	0.73	0.77
z_{12}	1.66	1.88*	1.85*
z_{23}	1.78	1.73 *	1.75*
z_{34}	1.73	1.75	1.76
z_{45}	1.71	1.74	1.77
z_{5-Cu1}	1.80	1.81	-

Table 4. Calculated absolute surface stress values and adsorbate-induced changes in the surface stress for Fe growth on W(110). Also shown are the experimental surface stress changes at the calculated coverages taken from the data of fig. 1. Experimental values are not given for the 2 ML film as this is judged not to be pseudomorphic.

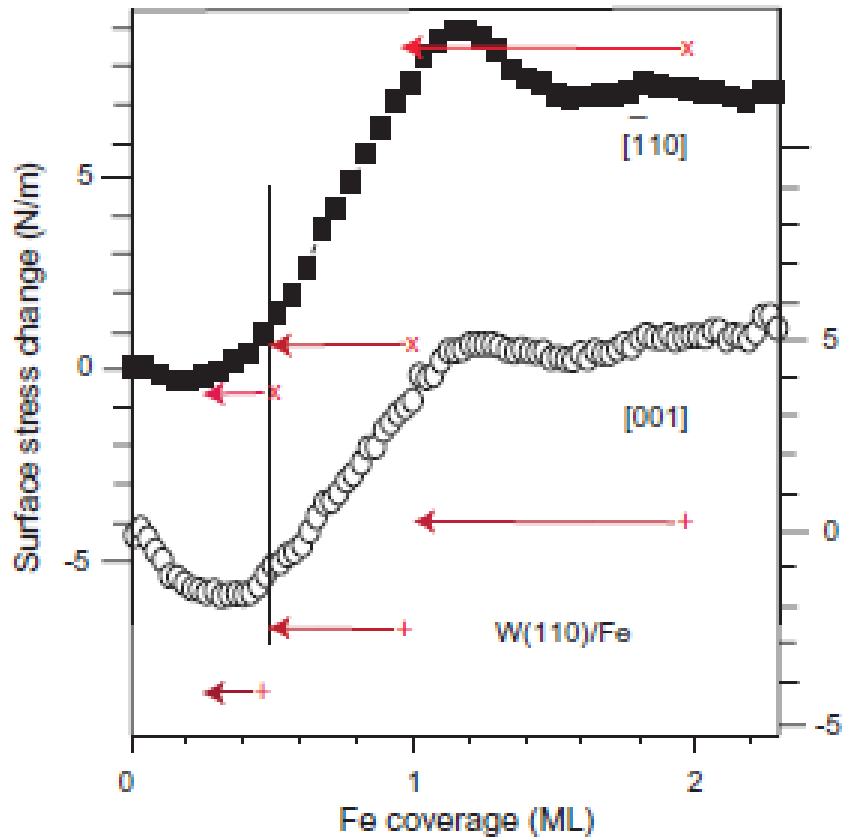| Surface	absolute surface stress (N/m) $[001]$, $[\bar{1}10]$	Calculated adsorbate-induced surface stress change (N/m) $[001]$, $[\bar{1}10]$	experimental adsorbate-induced surface stress change (N/m) $[001]$, $[\bar{1}10]$
W(110), clean	5.65, 3.75	-	-
W(110)c(2x2)-Fe (0.5 ML)	1.41, 3.07	-4.23, -0.68	-0.8, 0.7
W(110)(1x1)-Fe (1.0 ML)	2.98, 4.52	-2.66, 0.77	3.8, 7.5
W(110)(1x1)-Fe (2.0 ML)	5.86, 11.96	0.21, 8.21	-

Figure Caption

Fig. 1 Comparison of the experimental (filled squares and open circles) and calculated (plus and cross symbols) values of the surface stress change as a function of coverage for Fe growth on W(110). The experimental data are taken from ref [26]. The arrows illustrate the effect of a factor of two change in the coverage calibration.

References

1 H. Ibach, Surf. Sci. Rep. 29 (1997) 193

2 O. H. Nielsen, R. M. Martin, Phys. Rev. Lett. 50 (1983) 697

3 O. H. Nielsen, R. M. Martin, Phys. Rev. B 32 (1985) 3780

4 O. H. Nielsen, R. M. Martin, Phys. Rev. B 32 (1985) 3792

5 G. J. Aukland, M. W. Finnis, Phil. Mag. A 54 (1986) 302

6 R. J. Needs, Phys. Rev. Lett. 58 (1987) 53

7 D. Vanderbilt, Phys. Rev. Lett. 59 (1987) 1456

8 M.C. Payne, N. Roberts, R. J. Needs, M. Needels, J.D. Joannopoulos, Surf. Sci. 211/212 (1989) 1

9 R. J. Needs, M. J. Godfrey, M. Mansfield, Surf. Sci. 242 (1991) 215

10 P. Gumbsch, and M. S. Daw, Phys. Rev. B 44, 3934 (1991)

11 J. Wan, Y. L. Fan, D. W. Gong, S. G. Shen, and X. Q. Fan, Modelling Simul. Mater. Sci. Eng. 7, 189 (1999)

12 P. M. Marcus, X. Qian, W. Hübner, J. Phys.: Condens. Matter 12 (2000) 5541

13 Y. Yoshimoto, and S. Tsuneyuki, App. Surf. Sci. 237, 274 (2004)

14 P.J. Feibelman, Phys. Rev. B 56 (1997) 2175

15 S. Hong, A. Kara, T. S. Rahman, R. Heid, K. P. Bohnen, Phys. Rev. B 69 (2004) 195403

16 M. J. Harrison, D .P. Woodruff, J. Robinson, Surf. Sci. 572 (2004) 309

17 W. Pan, R. Popescu, H. L. Meyerheim, D. Sander, O. Robach, S. Ferrer, Minn-Tsong Lin, and J. Kirschner, Phys. Rev. B 71, 174439 (2005)

18 M.J. Harrison, D.P.Woodruff and J.Robinson, *Phys. Rev. B* **72** (2005) 113408

19 M.J. Harrison, D.P. Woodruff, J. Robinson, D. Sander, W. Pan, J. Kirschner, Phys. Rev. B 74 (2006) 165402

20 M.C. Payne, M.P. Teter, D.C. Allen, T.A. Arias and J.D. Joannopoulos Rev.Mod.Phys. 64 (1992) 1045

21 http://www.accelrys.com/cerius2/qmw.html

22 J. P. Perdew, K. Burke,M. Ernzerhof, Phys. Rev. Lett. 77 (1996) 3865

23 D. Sander, U. Linke, H. Ibach, Surf. Sci. 272 (1992) 318

24 D. Sander, A. Enders, C. Schmidthals, D. Reuter, J. Kirschner, Surf. Sci. 402-404 (1998) 351

25 M. Fuchs, M. Bockstedte, E. Pehlke, M. Scheffler, Phys. Rev. B 57 (1998) 2134

26 D. Sander, A. Enders, J. Kirschner, Europhys. Lett. 45 (1999) 208

27 W. Oed, H. Lindner, U. Starke, K. Heinz, K. Müller, J. B. Pendry, Surf. Sci. 224 (1989) 179

28 U. Starke, F. Bothe, W. Oed, K. Heinz, Surf. Sci. 232 (1990) 56

29 M. A. Van Hove, S. Y. Tong, Phys. Rev. Lett. 35 (1975) 1092

30 H. L. Meyerheim, D. Sander, R. Popescu, W. Pan, I. Popa, J. Kirschner, Phys. Rev. Lett. in press

31 J. Hong, R. Q. Wu, L. Lindner, E. Kosubek, K. Baberschke, Phys. Rev. Lett. 92 (2004) 147202

32 R. Nünthel, T. Gleitsmann, P. Poulopoulos, A. Scherz, J. Lindner, E. Kosubek, Ch. Litwinski, Z. LI, H. Wende, K. Baberschke, S. Stolbov, T. S. Rahman, Surf. Sci. 531 (2003) 53

33 C. Sorg, Pompandian, M. Bernien, K. Baberschke, H. Wende, R. Q. Wu, Phys. Rev. B 73 (2006) 064409

34 D. Sander, Rep. Prog. Phys. 62 (1999) 809

35 D. Sander, R. Skomski, A. Enders, C. Schmidthals, D. Reuter, J. Kirschner, J. Phys. D: Appl. Phys. 31 (1998) 663

36 H. L. Meyerheim, D. Sander, R. Popescu, J. Kirschner, P. Steadman, S. Ferrer, Phys. Rev. B 64 (2001) 045414